Molecular Microbiology (2015) 00(00), 00–00 ■
doi: 10.1111/mmi.13307
First published online 00 Month 2015

Expression of IroN, the salmochelin siderophore receptor, requires mRNA activation by RyhB small RNA homologues

Roberto Balbontín,[1†] Nicolás Villagra,[2] Maria Pardos de la Gándara,[1‡] Guido Mora,[2] Nara Figueroa-Bossi[1]* and Lionello Bossi[1]
[1]*Institute for Integrative Biology of the Cell (I2BC), CEA, CNRS, Université Paris-Sud, Université Paris-Saclay, 91198 Gif-sur-Yvette, France.*
[2]*Laboratorio de Patogénesis Molecular y Antimicrobianos, Facultad de Medicina, Universidad Andres Bello, Echaurren 183, Santiago, Chile.*

Summary

The *iroN* gene of *Salmonella enterica* and uropathogenic *Escherichia coli* encodes the outer membrane receptor of Fe^{3+}-bound salmochelin, a siderophore tailored to evade capture by the host's immune system. The *iroN* gene is under negative control of the Fur repressor and transcribed under iron limiting conditions. We show here that transcriptional de-repression is not sufficient to allow *iroN* expression, as this also requires activation by either of two partially homologous small RNAs (sRNAs), RyhB1 and RyhB2. The two sRNAs target the same sequence segment approximately in the middle of the 94-nucleotide 5′ untranslated region (UTR) of *iroN* mRNA. Several lines of evidence suggest that base pair interaction stimulates *iroN* mRNA translation. Activation does not result from the disruption of a secondary structure masking the ribosome binding site; rather it involves sequences at the 5′ end of *iroN* 5′ UTR. *In vitro* 'toeprint' assays revealed that this upstream site binds the 30S ribosomal subunit provided that RyhB1 is paired with the mRNA. Altogether, our data suggest that RyhB1, and to lesser extent RyhB2, activate *iroN* mRNA translation by promoting entry of the ribosome at an upstream 'standby' site. These findings add yet an additional nuance to the polychromatic landscape of sRNA-mediated regulation.

Accepted 9 December, 2015. *For correspondence. E-mail nara.figueroa@i2bc.paris-saclay.fr; Tel. (+33) 1 69823811; Fax (+33) 1 69823150. Present addresses: †Instituto Gulbenkian de Ciência, Oeiras, Portugal; ‡Laboratory of Microbiology and Infectious Diseases, The Rockefeller University, New York, New York, USA.

Introduction

Rewiring of gene expression networks in response to chemical or physical cues is central to the ability of bacterial pathogens to adapt to environmental changes. Adaptive responses can be finely tuned through the interplay of transcriptional and post-transcriptional regulators (Mandin and Guillier, 2013). Small non-coding RNAs (sRNAs) are key components of this regulatory circuitry (Gottesman and Storz, 2011). In gram-negative bacteria, a large family of sRNAs act by binding to chaperon protein Hfq and establishing short, often imperfect, base-pair interactions with target messenger RNAs (mRNAs). Hfq protects unpaired sRNAs against degradation by RNases and it is thought to facilitate mRNA recognition (De Lay *et al.*, 2013; Vogel and Luisi, 2011). The majority of Hfq binding sRNAs are negative regulators. Most members of this class target sequences within ribosome binding sites where formation of the RNA duplex obstructs the entry of the 30S ribosomal subunit, thereby inhibiting translation initiation. Translational repression is generally accompanied by the destabilization of both mRNA and sRNA (Massé *et al.*, 2003). On one hand, loss of ribosomal shielding renders the mRNA susceptible to internal attack by RNase E (Dreyfus, 2009). Conversely, the ability of Hfq to bind RNase E (Morita *et al.*, 2005) can promote the active recruitment of this enzyme near the site of the sRNA-mRNA association (Ikeda *et al.*, 2011) or even stimulate its activity at a distant site (Prevost *et al.*, 2011). Although a downstream event in all above pathways (Morita *et al.*, 2006), the RNase E step is important to make the sRNA action stoichiometric and irreversible. Finally, sRNA-mediated silencing can also proceed through instructed mRNA decay as opposed to translational inhibition. In the regulation of *Salmonella ompD* gene, the sRNA MicC pairs with internal sequences in the mRNA and guides RNase E to cleave the mRNA at a position adjacent to the pairing site (Bandyra *et al.*, 2012).

Small RNAs can also activate gene expression, typically by stimulating translation initiation. The paradigmatic

example is represented by the *rpoS* mRNA whose 5′ UTR folds into a secondary structure that sequesters the Shine-Dalgarno (SD) motif causing the translation initiation step to be intrinsically inefficient. Any of three different sRNAs, can counter this effect by establishing an alternative pairing configuration that frees the ribosome-binding site thus activating translation (McCullen *et al*., 2010; Soper *et al*., 2010). More recently, a number of alternative sRNA-mediated activating mechanisms have emerged (reviewed in Papenfort and Vanderpool, 2015). One system features a direct competition between Hfq, acting as a translational repressor, and the sRNA, which upon pairing with the target sequence redirects Hfq to a different site (Salvail *et al*., 2013). Other mechanisms are independent of translation and rely on the sRNA preventing or slowing down degradation of the mRNA (Papenfort *et al*., 2013; Frohlich *et al*., 2013).

The data described in this paper point to the existence of a further variation in the RNA-dependent activation theme, whereby the sRNA stimulates translation of the target gene by facilitating ribosomal recruitment at an upstream 'standby' site. This mechanism was uncovered during a study of the regulation of iron uptake in *Salmonella*.

To acquire iron from the environment, most free-living microorganisms synthesize and secrete a class of organic molecules named siderophores, which capture ferric ion from organic or inorganic sources (reviewed in Crosa and Walsh, 2002; Fischbach *et al*., 2006; Wandersman and Delepelaire, 2004). The iron-siderophore complex is then imported into the cell through high affinity receptors (Braun and Braun, 2002; Braun and Hantke, 2011). Enterobactin, the archetypal siderophore of enterobacterial species like *Escherichia coli* and *Salmonella enterica*, is synthesized through a pathway that branches off from the biosynthetic pathway of aromatic amino acids and is carried out by the products of the *ent* genes. Enterobactin export involves the functions of EntS (Furrer *et al*., 2002) and TolC (Bleuel *et al*., 2005) while the import of its iron-bound form occurs through the high affinity, TonB-gated FepA receptor (Buchanan *et al*., 1999). Siderophore function is crucial for proliferation of bacterial pathogens in animal fluids and tissues where iron is sequestered by lactoferrin, transferrin and proteins alike (Schaible and Kaufmann, 2004). Enterobactin is ill-suited as an iron scavenger in these microenvironments due to its hydrophobicity and susceptibility to lipocalin-2, an innate immune response protein that specifically traps ferric enterobactin (Flo *et al*., 2004). *Salmonella* and uropathogenic *Escherichia coli* strains circumvent this problem by synthesizing and secreting salmochelin, a glycosylated variant of enterobactin that is more hydrophilic and refractory to lipocalin-2 binding (Fischbach *et al*., 2006; Muller *et al*., 2009). This pathway originates from the horizontal acquisition of the *iroA* locus, which comprises the *iroBCDE* operon and the adjacent, convergently oriented *iroN* gene (Bäumler *et al*., 1998). The *iroBCDE* operon encodes functions involved in salmochelin synthesis and export; IroN is the outer membrane receptor through which ferric salmochelin is internalized (Bäumler *et al*., 1998; Hantke *et al*., 2003). The relevance of this pathway in pathogenicity was highlighted by the finding that the *iroBCDE iroN* locus confers a competitive advantage to *Salmonella* in colonizing the inflamed intestine of wild-type mice but not of mice deficient in lipocalin-2 production (Raffatellu *et al*., 2009). Once delivered to the periplasm through the respective receptors, Fe^{3+}-enterobactin and Fe^{3+}-salmochelin are chaperoned by FepB to the FepDGC transporter and translocated to the cytoplasm where they are degraded by the Fes and IroD hydrolases, respectively (Lin *et al*., 2005; Zhu *et al*., 2005; Crouch *et al*., 2008). The iron released from hydrolyzed siderophores is transferred to bacterial proteins and ligands. At some point along these processes, some reduced iron is produced and maintained in a soluble form. The size of this labile Fe^{2+} pool is tightly regulated to limit the harmful effects of Fenton chemistry. Fe^{2+} levels are controlled homeostatically through modulation of iron uptake and allocation.

In *Escherichia coli*, iron homeostasis is achieved through the interplay of two global regulators: the Fur protein and RyhB small RNA. Fur is a Fe^{2+}-binding polypeptide that, upon undergoing Fe^{2+}-dependent dimerization, binds specific DNA sequences (Fur boxes) in the promoter regions of iron uptake genes and represses transcription (Carpenter *et al*., 2009; Hantke, 2001). A decline in Fe^{2+} levels shifts the equilibrium towards Fe^{2+}-free Fur monomers, resulting in the progressive relief of repression. Included in the Fur regulon is the gene for RyhB sRNA. Accumulating under iron-limiting conditions, RyhB downregulates the synthesis of a number of non-essential iron-utilization and iron-storage proteins (including superoxide dismutase SodB and bacterioferritin Bfr) by pairing with and destabilizing the corresponding mRNAs (reviewed in Massé *et al*., 2007). In doing so, RyhB limits iron consumption when the latter becomes scarce. This activity, referred to as 'iron sparing' directly impacts the intracellular concentration of chelatable iron (Jacques *et al*., 2006; Massé *et al*., 2005).

RyhB can also activate gene expression. This is the case of the *shiA* gene, which encodes the permease for shikimate, an enterobactin precursor. Activation of *shiA* expression by RyhB was ascribed to the sRNA-mediated disruption of a secondary structure inhibiting ribosome binding to *shiA* mRNA (Prevost *et al*., 2007). Further positive effects of RyhB on enterobactin

synthesis and transport result from direct stimulation of *entCEBAH* expression through an unknown mechanism and, indirectly, from its repression of *cysE* mRNA translation. This last effect was rationalized considering that the *cysE* gene product, serine acetyl transferase, diverts serine from enterobactin biosynthesis (Salvail *et al*., 2010). The relevance of RyhB function in siderophore production and virulence was recently substantiated in uropathogenic *Escherichia coli* (Porcheron *et al*., 2014).

In *Salmonella enterica*, the Fur regulon includes, among others, the *iroBCDE iroN* locus and two *ryhB* gene homologs, an 83% identical ortholog (95 bp long) at the same chromosomal position as the *ryhB* gene of *Escherichia coli*, and a 64% identical paralog (97 bp) inside a genomic island (Padalon-Brauch *et al*., 2008). These two sRNAs have been variably called RyhB and IsrE (Padalon-Brauch *et al*., 2008), RfrA and RfrB (Leclerc *et al*., 2013; Ellermeier and Slauch, 2008) and RyhB-1 and RyhB-2 (Calderón *et al*., 2014; Kim and Kwon, 2013; Ortega *et al*., 2012). The latter terminology was adopted in this study. We show here that RyhB1 and RyhB2 activate *iroN* expression at the post-transcriptional level by pairing with a sequence in the middle of the leader region of *iroN* mRNA.

Results

IroN is regulated by Hfq

While comparing the outer membrane protein (OMP) profiles from wild-type *Salmonella* and from a strain lacking sRNA-binding protein Hfq in polyacrylamide gels, we noticed that OMP preparations from cells grown in minimal medium contained a cluster of closely-migrating high-molecular weight bands that were absent in cells grown in LB (Fig. 1A). To determine the identity of these proteins, bands were excised from the gel (see Supporting Information Fig. S1) and subjected to MALDI-TOF analysis (see Experimental procedures). This work identified three siderophore receptor proteins: enterochelin receptor FepA, salmochelin receptor IroN and ferrichrome receptor FhuA (Figs. 1A and Supporting Information Fig. S1). These findings suggested that the influence of the growth medium on the occurrence of the three proteins was in relation with iron concentration; namely, iron levels in LB might be high enough to cause full repression of *fepA, iroN* and *fhuA* genes by Fur (Bäumler *et al*., 1998; Tsolis *et al*., 1995). Consistent with this interpretation, the FepA/IroN/FhuA band cluster became readily detectable when the OMP preparation was made from LB-grown cells of a strain carrying a deletion of the *fur* gene (Fig. 1A). Intriguingly, the relative abundance of FepA and IroN differed substantially between wild-type and the *hfq* mutant (Supporting Information Fig. S1), suggesting that either protein, or both, could be regulated by Hfq. To assess this regulation, *lacZ* translational fusions to the initial portions of *fepA* and *iroN* coding sequences were constructed by chromosomal recombineering and *lacZ* expression compared in Δ*fur* strains carrying or lacking the *hfq* gene. Results showed the two fusions to exhibit markedly different responses. While the *fepA-lacZ* fusion did not change significantly, expression of the *iroN-lacZ* fusion showed a sharp fivefold reduction in the absence of Hfq (Fig. 1B). These results suggested that *iroN* might be up-regulated by a Hfq-dependent small RNA.

RyhB1, and to lesser extent RyhB2, activate iroN *expression*

Considering that RyhB1 and RyhB2 were the most likely candidates for this regulation (see Introduction), we deleted the *ryhB1* and/or *ryhB2* genes and analyzed the effects of these deletions on OMP profiles in a *fur* deficient background. Lack of RyhB1 alone caused a slight decrease in the intensity of the IroN band, whereas the pattern from the strain lacking RyhB2 was indistinguishable from wild-type. However, removal of both *ryhB1* and *ryhB2*, strongly reduced IroN accumulation (Fig. 1C). Measurement of ß-galactosidase activity in strains carrying the *iroN-lacZ* fusion confirmed the above trend. LacZ levels were fourfold to fivefold lower in a strain lacking both RyhB1 and RyhB2 as compared to wild-type or to the single RyhB2 deletion mutant (Fig. 1D). Again, the RyhB1 mutant appeared affected in this test, suggesting that RyhB2 cannot fully replace RyhB1 in stimulating *iroN* expression. Finally, in strains where the translated portion of *iroN* is replaced by the open reading frame (orf) of an epitope-tagged *cat* gene, accumulation of the Cat protein was markedly reduced in the *ryhB1 ryhB2* doubly deleted background but not in the single Δ*ryhB2* mutant (Fig. 1E). Altogether, these results indicate that RyhB1, and to a lesser extent RyhB2, up-regulate *iroN*. Furthermore, the data suggest that the target sequence of this regulation lies entirely within the 5′ untranslated region (5′-UTR) of *iroN* mRNA.

RyhB1 up-regulates IroN by base-pairing with a sequence 44 nt upstream of the translation initiation codon of iroN mRNA

The 5′ end of the *iroN* mRNA was mapped by primer extension (Supporting Information Fig. S2). Presence of a sequence with high similarity to a Fur box immediately

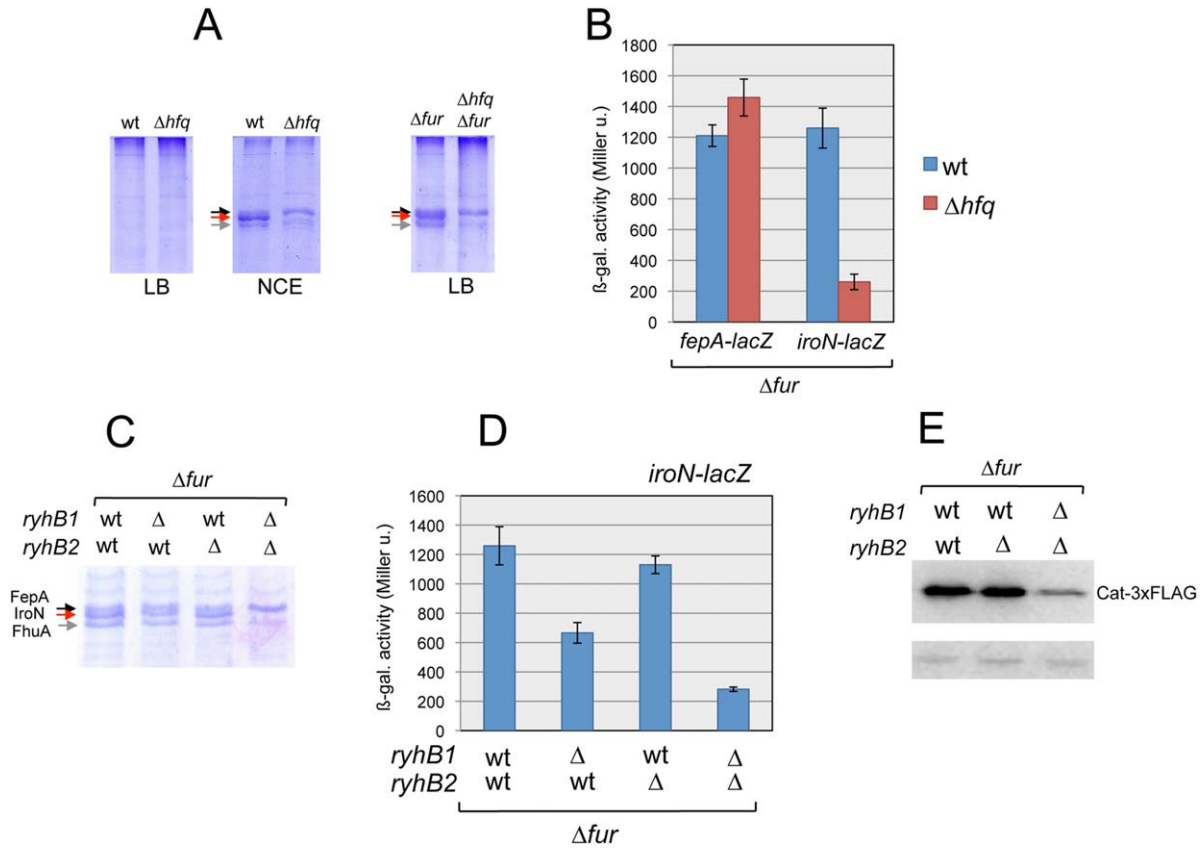

Fig. 1. Requirement for Hfq-dependent small RNAs in the expression of Fur-controlled IroN receptor.
A. Analysis of outer membrane proteins from wild-type and Δ*hfq* mutant strains of *Salmonella*. Cultures of strains MA3409 (wt), MA7791 (Δ*hfq*), MA9980 (Δ*fur*) and MA10133 (Δ*hfq* Δ*fur*) were grown in minimal medium (NCE, 0.2% glycerol) or in rich medium (LB) at 37°C and processed for OMP preparation as described in Experimental procedures. Proteins were separated by SDS-PAGE on a 12% gel. Only the upper portion of the gel is shown. The bands denoted by black, red and gray arrows were analyzed by mass spectrometry and identified as siderophore receptors FepA, IroN and FhuA, respectively (see text).
B. Effect of deleting *hfq* on the expression of *lacZ* translational to *fepA* and *iroN* genes. The *lacZ* orf is fused to the 9th codon of *fepA* and to the 5th codon of *iroN*. Fusions were constructed in the chromosome as described in Experimental procedures. Strains MA10185 (*fepA-lacZ* Δ*fur*), MA10187 (*fepA-lacZ* Δ*fur* Δ*hfq*), MA10954 (*iroN-lacZ* Δ*fur*) and MA11573 (*iroN-lacZ* Δ*fur* Δ*hfq*) were grown to late exponential phase and assayed for ß-galactosidase activity (Experimental procedures).
C. Analysis of OMPs from strains carrying or lacking the *ryhB1* and/or *ryhB2* genes. Cultures from strains MA9980 (Δ*fur*), MA10169 (Δ*ryhB1*), MA10170 (Δ*ryhB2*) and MA10171 (Δ*ryhB1* Δ*ryhB2*) were grown in LB medium and processed as in A.
D. Effects of *ryhB1* and/or *ryhB2* deletions on the expression of *iroN-lacZ*. Strains MA10954 (*iroN-lacZ* Δ*fur*), RB116 (*iroN-lacZ* Δ*fur* Δ*ryhB1*), MA10430 (*iroN-lacZ* Δ*fur* Δ*ryhB2*), and MA10431 (*iroN-lacZ* Δ*fur* Δ*ryhB1* Δ*ryhB2*) were cultured and assayed for ß-galactosidase activity as in B.
E. Western blot analysis of strains expressing epitope-tagged *cat* gene fusions to *iroN* 5′ UTR. A strain with the entirety of the *iroN* orf deleted and replaced by the orf of a C-terminal *cat*–3xFLAG fusion was constructed by DNA recombineering (Supporting Information Tables S2 and S3) and used to produce strains MA11734, MA11735 and MA11736 (Supporting Information Table S1). Overnight cultures of these three strains were processed for Western blot analysis as described in Experimental procedures. A weak non-specific signal (bottom strip) provides a loading control. The full genotypes of all strains above are listed in Supporting Information Table S1.

upstream from the 5′-end strongly suggested that this position corresponds to the transcription start site (Fig. 2A). A second putative Fur box spans the transcribed interval between the +8 and +26. At the beginning of this study, doubt existed as to which of two in-frame AUG triplets found at positions +89 and +95 constituted the *iroN* translation initiation codon (denoted by wavy overlines in Fig. 2A). To clarify this point, each one of the two AUG codons was separately mutagenized in the *iroN-lacZ* fusion context and the phenotype of strains carrying these constructs in a Δ*fur* background scored on lactose indicator plates. Only the strain in which the AUG at +95 was unmodified expressed ß-galactosidase activity, conclusively identifying this triplet as the functional initiation codon (Supporting Information Fig. S3A).

Examination of the sequence of *iroN* 5′ UTR identified a segment complementary to a sequence found in both RyhB1 and RyhB2 (Fig. 2B). To assess the role of these elements in the regulation, reciprocal dinucleotide

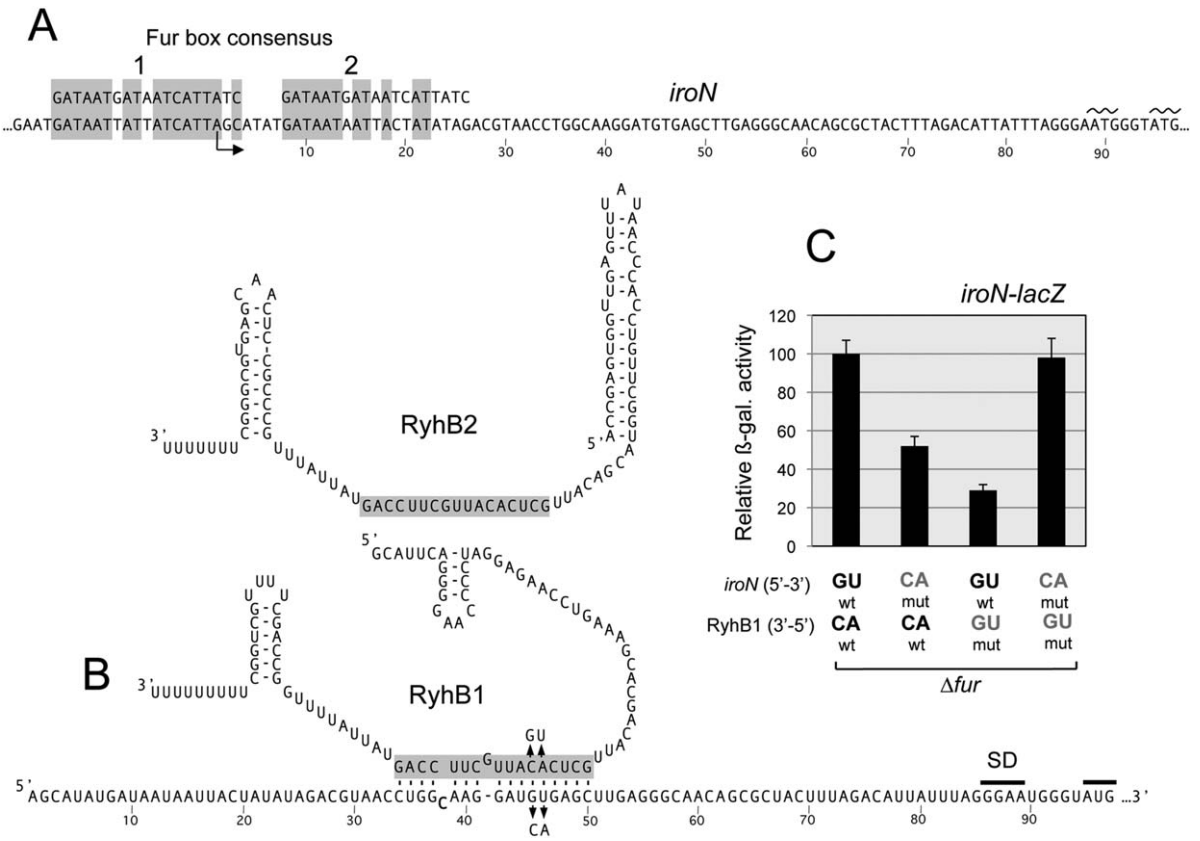

Fig. 2. RyhB1 activates *iroN* expression by base-pairing with a sequence in the middle of the *iroN* 5′ UTR.
A. DNA sequence of the promoter-proximal portion of the *iroN* gene (sense strand). Shaded boxes indicate sequences showing identity with the consensus sequence for the Fur binding site. Wavy overlines denote in-frame ATG triplets encoding putative translation initiation codons.
B. Both RyhB1 and RyhB2 contain a sequence segment (shaded box) partially complementary to a sequence in the middle of *iroN* 5′ UTR. Double base changes at adjacent positions (+45,+46) within this portion of *iroN* (GpU to CpA), as well as reciprocal changes in the presumptive pairing nucleotides in RyhB1, were introduced by site-directed chromosomal mutagenesis (Experimental procedures; Supporting Information Tables S2 and S3).
C. ß-galactosidase activity in strains carrying *lacZ* translational fusions to wild-type and mutant alleles of *iroN* 5′ UTR in the presence or absence of compensatory mutations in the *ryhB1* gene. Strains used were MA10430, MA10457, MA10514 and MA10513 (Supporting Information Table S1).

changes were introduced at the presumptive pairing positions of *iroN* and *ryhB1* and their effects on *iroN-lacZ* expression measured in a Δ*fur* Δ*ryhB2* background. As shown in Fig. 2C, while separately each of the mutations reduces *iroN* activation, combining them in the same strain restores nearly normal levels of expression. This provides compelling genetic evidence that RyhB1 up-regulates *iroN* through the establishment of a base-pairing interaction.

An implication of the above findings is that *iroN* derepression under iron limiting conditions can occur only after that RyhB1 has sufficiently accumulated. Consistent with this idea, measurement of *iroN-lacZ* and *fepA-lacZ* induction rates in the presence of increasing concentrations of iron chelator dipyridyl showed that *iroN* exhibits a markedly delayed response to iron limitation, derepressing only under severe iron depletion (Supporting Information Fig. S3B).

RyhB1 expression is important for iroN *mRNA stability*

Northern blot hybridization experiments were performed to examine the effects of the *ryhB1* and *ryhB2* deletions in strains with a wild-type *iroN* locus. The results in Fig. 3A show that full-length *iroN* mRNA is present at comparable levels in wild-type and in the Δ*ryhB2* mutant while it is nearly or completely undetectable in strains lacking RyhB1 or both RyhB1 and RyhB2. Thus, as already inferred from measuring *iroN-lacZ* fusion expression, the contribution of RyhB2 to *iroN* regulation is smaller than RyhB1's. This is possibly ascribable to a lower accumulation of RyhB2, compared to RyhB1, in cells growing exponentially in LB (Fig. 3B). Interestingly, if one takes into account its reduced levels, RyhB2 appears comparatively more efficient than RyhB1 in down-regulating *sodB* mRNA. As shown in Fig. 3A, *sodB* mRNA accumulates to a much greater extent in the Δ*ryhB1* Δ*ryhB2* strain

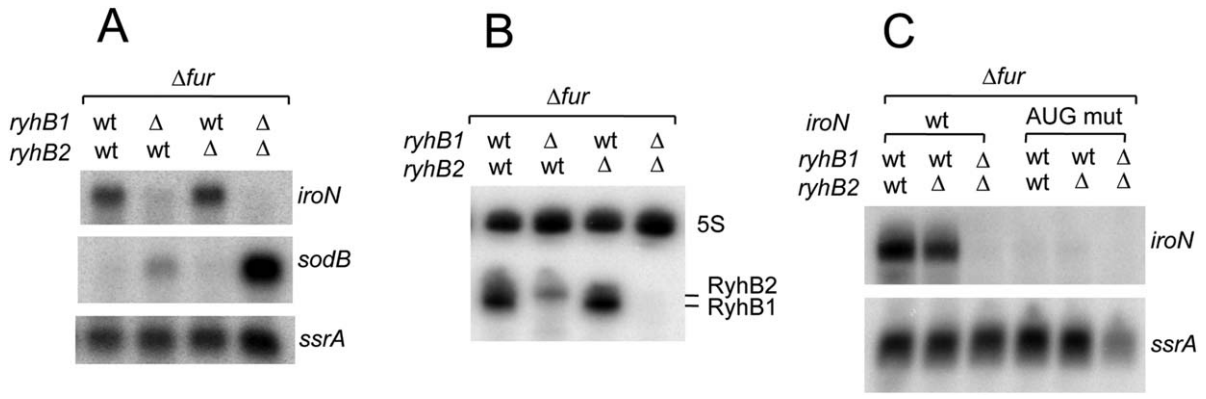

Fig. 3. RyhB1 counters *ironN* mRNA degradation provided that *ironN* mRNA is translated.
A. Northern blot analysis of *ironN* and *sodB* mRNAs in strains carrying or lacking *ryhB1* and/or *ryhB2*. RNA extracted from exponentially growing cultures in LB medium (OD_{600} = 0.35) of strains MA9980 (Δ*fur*), MA10169 (Δ*fur* Δ*ryhB1*), MA10170 (Δ*fur* Δ*ryhB2*) and MA10171 (Δ*fur* Δ*ryhB1* Δ*ryhB2*) was fractionated on a 1% agarose-formaldehyde gel, transferred to a nylon membrane and the blot was sequentially hybridized with ^{32}P-labelled DNA oligonucleotides ppF37 (*ironN*) and ppI70 (*sodB*). Hybridization with probe pp813, specific for tmRNA (*ssrA*), provided an internal standard.
B. Quantification of sRNA levels. RNA from strains in A was fractionated on a 8% polyacrylamide-urea gel, electroblotted onto a nylon membrane and the blot hybridized with ppE18, a DNA probe specific for both RyhB1 and RyhB2, and ppB10 specific for 5S RNA.
C. Analysis of the effects of an initiation codon mutation on *ironN* mRNA levels in strains carrying wild-type or deleted versions of *ryhB1* or of *ryhB1* and *ryhB2*. RNA was extracted from strains MA9980, MA10170, MA10171, MA12026, MA12030 and MA12032 (Supporting Information Table S1) and analyzed as in A. The last three strains harbor allele *ironN*[T96A,G97C], which changes *ironN* initiation codon, AUG, to AAC (Experimental procedures, Supporting Information Tables S2 ad S3). The Northern blot was hybridized with ppF37 and pp813 (see above).

than in either of the two single mutants. Examination of the putative pairing regions of the two sRNAs reveals that the portions interacting with *sodB* and *ironN* mRNA are nonidentical and that RyhB2's complementarity to *sodB* mRNA is slightly more extended than RyhB1's (Supporting Information Fig. S4). This could make RyhB2 more efficient at repressing the gene.

One way to explain the positive effect of RyhB1 and RyhB2 on *ironN* expression is to say that the two sRNAs stimulate *ironN* mRNA translation. The instability of *ironN* mRNA in Δ*ryhB1* Δ*ryhB2* strain would then be a consequence of its inefficient translation. This interpretation predicts that preventing *ironN* mRNA translation should cause the mRNA to become unstable even in the presence of RyhB1 and RyhB2. The prediction was tested analyzing the *ironN* mRNA patterns in a strain with the *ironN* initiating AUG codon changed to AAC. As shown in Fig. 3C, the *ironN* mRNA is no longer detected in the initiator codon mutant in the *ryhB1*$^+$ *ryhB2*$^+$ background confirming that the mRNA is rapidly degraded if not translated.

RNases act downstream in the regulatory pathway

Poorly translated mRNA are often especially susceptible to cleavage by RNase E (Dreyfus, 2009). We therefore tested whether this ribonuclease was responsible for the instability of *ironN* mRNA in cells lacking RyhB1 and RyhB2. RNase E being an essential enzyme, the experiment was performed using the temperature sensitive *rne-3071* allele (Figueroa-Bossi *et al.*, 2009). A 15 min treatment at 43°C restored *ironN* mRNA accumulation in cells carrying *ryhB1* and *ryhB2* deletions in combination with *rne-3071* (Fig. 4A, compare lanes 2 and 6) confirming the primary role of RNase E in the degradation process. The *rne-3071* mutation also causes a net increase in *ironN* transcript (compare lanes 1 and 5) suggesting that RNase E participates in the normal turnover of this mRNA (i.e., even when the mRNA is optimally expressed).

An alternative mechanism by which RyhB1 and RyhB2 could up-regulate *ironN* expression is by directly interfering with RNase E activity (Papenfort and Vanderpool, 2015). In particular, if RNase E began processing the transcript from the 5′ end, the sRNA:mRNA hybrid could protect the mRNA against cleavage. The 5′ entry pathway of RNase E relies on the removal of triphosphate by the RppH nuclease (Deana *et al.*, 2008). Thus, we initially tested if inactivating RppH altered *ironN* regulation. We constructed an *rppH* gene deletion and analyzed its effects on *ironN* mRNA levels and on expression of *ironN-lacZ* fusion. Both types of measurements showed no significant differences between wild-type in the *rppH* mutant (data not shown).

Next, we tested whether RyhB1 and RyhB2 were still active in regulation under conditions of RNase E inactivation. Cells carrying *rne-3071*, the *ironN-lacZ* fusion and either wild-type or deleted versions of *ryhB1* and *ryhB2* were incubated at 43°C prior to inducing iron starvation by addition of 2,2′ dipyridyl. Accumulation of ß-galactosidase activity from the derepressed *ironN-lacZ* fusion was measured following a further 1 h incubation at 43°C. ß-

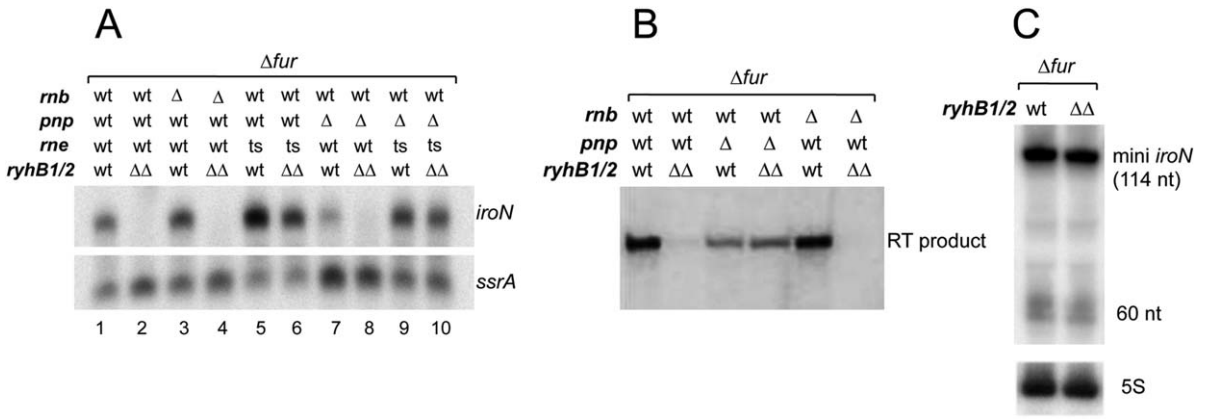

Fig. 4. RNase E and PNPase participate in the degradation of *iroN* mRNA.
A. Northern blot analysis of *iroN* mRNA in strains carrying wild-type or deleted versions of *ryhB1* and *ryhB2* in combination with wild-type and mutant alleles of ribonucleases. Strains RB41, RB42, RB45, RB46, RB57, RB58, RB43, RB44, RB59 and RB60 (Supporting Information Table S1) were grown in LB at 37°C to mid exponential phase. The cultures from strains carrying the temperature-sensitive *rne-3071* allele (RB57, RB58, RB59, RB60) were shifted to 43°C to for 15 min prior to RNA extraction. RNA was extracted as described in Experimental procedures and subjected to Northern blot hybridization as in Fig. 3A. Note: for unknown reasons, the *pnp* deletion could not be obtained in *Salmonella* strain LT2 and was isolated in strain ATCC14028. Hence, all strains above were derived from strain ATCC14028 (see Supporting Information Table S1 for the complete genotypes).
B. Analysis of *iroN* mRNA by primer extension. RNA extracted from exponentially growing cultures of strains MA9980, MA10171, RB43, RB43, RB44, RB45 and RB46 (Supporting Information Table S1), was used as template for reverse transcription with a ^{32}P-labelled primer (ppH09; Supporting Information Table S2) annealing inside *iroN* coding sequence (+124 to +143). Reaction products were analyzed on a 10% polyacrylamide-urea gel. A single extension product was obtained. Only the portion of gel containing this band is shown.
C. Northern blot analysis of an *iroN*-derived mini transcript. Strains MA11656 (Δ*fur*) and MA11672 (Δ*fur* Δ*ryhB1* Δ*ryhB2*) carry a shortened version of the *iroN* gene in which the orf portion of the gene is replaced by the sequence of a Rho-independent transcription terminator (Supporting Information Tables S1 and S3). RNA from these strains was fractionated on a 8% polyacrylamide-urea gel, electroblotted onto a nylon membrane and the blot was hybridized with oligonucleotides ppN12 (*iroN*) and ppB10 (5S RNA) (Supporting Information Table S2).

galactosidase accumulated at a significantly higher level in the *ryhB1*$^+$ *ryhB2*$^+$ strain than in the Δ*ryhB1* Δ*ryhB2* derivative, strongly suggesting that sRNA-mediated stimulation of *iroN* expression is independent of RNase E activity (Supporting Information Fig. S5).

In parallel to the above analysis, primer extension experiments were performed to assess the occurrence of endonucleolytic cleavages in *iroN* 5′ UTR. As the template RNA to be used for these experiments could be affected by the activity of 3′ exonucleases, some RNA preparations were made from strains deleted for the genes encoding PNPase (*pnp*) and RNase II (*rnb*). The only significant extension product detected in this experiment corresponded to the 5′ end of full-length *iroN* mRNA (Fig. 4B). This band was obtained with template RNA from wild-type and *rnb* mutant but not from the Δ*ryhB1* Δ*ryhB2* derivatives of these strains. Interestingly, the primer extension product was present in comparable amounts in the *ryhB1*$^+$ *ryhB2*$^+$ and Δ*ryhB1* Δ*ryhB2* derivatives of the Δ*pnp* mutant (Fig. 4B). We interpret these findings to suggest that lack of RyhB1 and RyhB2 causes *iroN* mRNA to be cleaved internally, presumably by RNase E and the cuts serve as entry sites for PNPase which degrades the RNA through its 3′ to 5′ exonuclease activity. Therefore, like RNase E, PNPase acts downstream in the regulatory pathway. Consistent with this conclusion, the Δ*pnp* deletion does not confer stability to the full-length *iroN* transcript (Fig. 4A, compare lanes 2 and 8) nor restores the full expression of the *iroN-LacZ* fusion in the Δ*ryhB1* Δ*ryhB2* background (Supporting Information Fig. S6A). In fact, the data in Supporting Information Fig. S6A also show that the *pnp* deletion prevents full activation of *iroN-lacZ* in the presence of wild-type *ryhB1* and r*yhB2* alleles. This effect can be ascribed to the lower levels of RyhB1 in the Δ*pnp* mutant (Supporting Information Fig. S6B), a finding already reported for the *Escherichia coli* RyhB (De Lay and Gottesman, 2011). Confirming these previous data, the RyhB1 decrease in the Δ*pnp* background was suppressed by inactivating RNase E (Supporting Information Fig. S6B).

As an alternative approach to detect RNA cleavages in *iroN* 5′UTR, the gene segment downstream from position +88 was deleted and replaced by the Rho-independent transcription terminator of the *glnS* gene. The resulting 114 nt mini transcript was visualized by Northern blot hybridization following separation in polyacrylamide gel. No major differences were observed in the levels of *iroN*-derived RNA or in the pattern of putative processing intermediates between the strains carrying or lacking RyhB1 and RyhB2 (Fig. 4C). The apparent requirement for the translated portion of the *iroN* mRNA in order to observe the sRNA-dependent

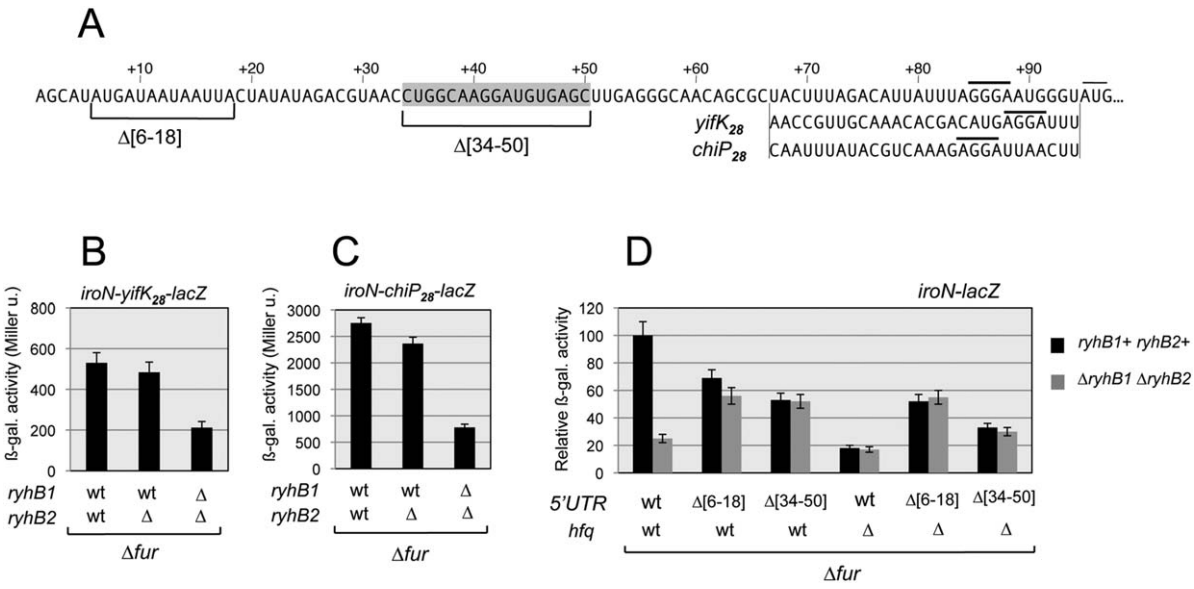

Fig. 5. Role of *iroN* 5′UTR sequences in RyhB1-mediated activation.
A. Sequence changes in *iroN* 5′ UTR. All mutants were obtained by chromosomal DNA recombineering (Supporting Information Tables S3). Alleles *iroN*::*yifK*$_{28}$ and *iroN*::*chiP*$_{28}$ replace the 28 nucleotides immediately preceding *iroN* AUG codon with the corresponding sequence from the *yifK* and *chiP* genes (see text for details).
B and C. Effects of *iroN*::*yifK*$_{28}$ (B)and *iroN*::*chiP*$_{28}$ (C) on the regulation of the *iroN-lacZ* fusion. ß-galactosidase activity was measured in strains carrying either *iroN*::*yifK*$_{28}$ (MA11639, MA11640 and MA11641) or *iroN*::*chiP*$_{28}$ (MA11679, MA11680, MA11681) in the *lacZ* fusion context and either wild-type or deleted versions of *ryhB2* or of *ryhB1* and *ryhB2*. Moreover, the two sets of strains are deleted for the genes for the sRNAs GcvB and ChiX which target sequences inside *yifK* and *chiP* replacement segments, respectively (see Supporting Information Table S1 for full genotypes).
D. RyhB1 activates *iroN* by overriding an inhibitory effect of the A/U rich region. ß-galactosidase assays were performed on strains MA10954, MA10431, RB124, RB125, RB104, RB105, MA11573, MA11561, MA11587, MA11588, MA11674 and MA11675 (Supporting Information Table S1).

differences in mRNA stability further supported the notion that RyhB1 and RyhB2 act by stimulating *iroN* translation as opposed to impeding mRNA degradation.

RyhB1/2 activity is independent of the sequence of the ribosome binding site

Envisaging that translational activation by RyhB1/2 might involve the disruption of secondary structures in the ribosome binding region (see Introduction), we initially focused on this aspect. Analysis by the Mfold program (Zuker, 2003) showed the potential for the *iroN* leader sequence to fold into a secondary structure in which the sequence immediately upstream of the SD element base pairs with a portion of the RyhB target sequence (Supporting Information Fig. S7A). Conceivably, this structure might sequester the ribosome binding site (RBS) and the RyhB1 interaction be required to disrupt this conformation. If so, mutations disrupting intramolecular pairing should activate *iroN* expression, at the same time relieving the dependence on RyhB1. The prediction was tested by introducing multiple nucleotide changes on the 5′ side of the SD sequence and measuring the effects on the expression of the *iroN-lacZ* fusion. Results showed that while contributing to overall translation initiation efficiency, the mutated region plays no significant role in RyhB1/2-dependent regulation (Supporting Information Fig. S7B,C). Thus these data failed to substantiate the role of the structure in Supporting Information Fig. S7A. Finally, a 28 nt segment immediately preceding the *iroN* AUG initiation codon was replaced by the corresponding region from two separate genes being studied in the laboratory, *yifK* (Yang *et al*., 2014) and *chiP* (Figueroa-Bossi *et al*., 2009) (see Fig. 5A). Constructs were made in the background of the *iroN-lacZ* fusions and regulation assessed by measuring ß-galactosidase activity. As shown in Fig. 5B and C, although the substitutions affect the basal levels of expression, RyhB1-mediated regulation is maintained in the two constructs. These findings strongly suggest that the determinants of the regulation lie outside the replaced segment, presumably on its upstream side. Thus, regulation by RyhB does not involve releasing the RBS from an inhibitory structure but likely occurs by an alternative mechanism.

RyhB1/2 stimulates ribosome binding to an upstream site in vitro

The effects of RyhB1 on the binding of the 30S ribosomal subunit to *iroN* mRNA were assessed *in vitro* by

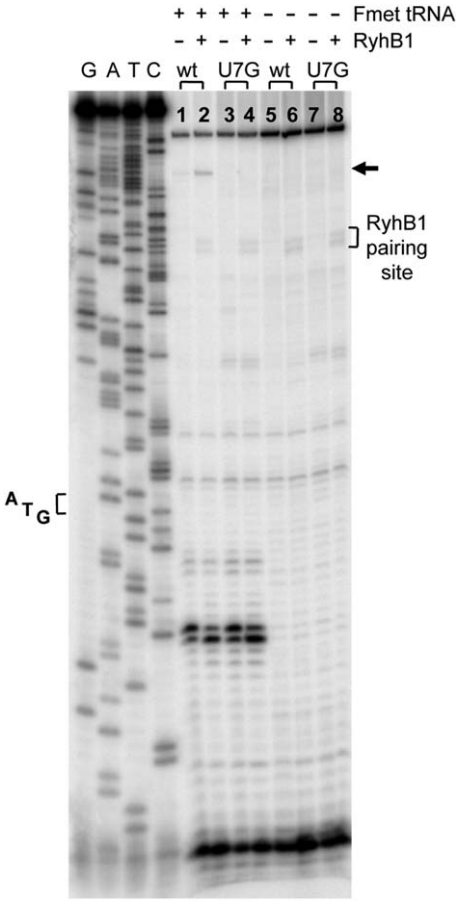

Fig. 6. RyhB1 stimulates binding of the 30S ribosomal subunit at the 5′ of *iroN* mRNA *in vitro*. Full-length RyhB1 RNA and the portion of *iroN* mRNA from +1 to +188 were obtained by *in vitro* transcription with T7 RNA polymerase. Templates were generated by PCR amplification of chromosomal DNA with primers ppI63 and ppI64 (RyhB1), ppI46 and ppH10 (*iroN* wt) and ppI80 and ppH10 (*iroN* U7G). Reverse transcription was primed with oligonucleotide ppH09 (Supporting Information Table S2). Toeprint analysis was performed as described in Experimental procedures. An arrow denotes an f-Met tRNA-dependent complex forming at the 5′ end of the mRNA.

the toeprinting technique (Hartz *et al.*, 1988). This analysis detected a major signal, in the form of a double band, at the position corresponding to the translation initiation site. As shown in Fig. 6, RyhB1 does not significantly affect the overall intensity of the signal (note, the apparent differences in band ratios were not reproduced in separate experiments). Intriguingly, a second, highly reproducible toeprint signal is visible in the upper portion of the gel and markedly enhanced by the presence of RyhB1 (compare upper band in lanes 1 and 2). The toeprint position would be consistent with a 30S subunit forming a ternary complex at an AUG triplet between +6 and +8 (Fig. 5A). To confirm this, the experiment was repeated with a mutant in which the 5′-end AUG is changed to AGG (allele U[+7]G). The change completely eliminated the upstream signal (Fig. 6, lanes 3 and 4). Since this effect could explain RyhB1-mediated regulation of *iroN in vivo*, we introduced the U[+7]G allele in the chromosome and measured ß-galactosidase in strains carrying the *iroN-lacZ* fusion in the presence or absence of *ryhB1* (in a *ryhB2*-deleted background). Results showed that RyhB1 still up-regulates *iroN-lacZ* in the U[+7]G mutant to an extent indistinguishable from wild-type (Supporting Information Fig. S8). Thus, the results ruled out a role of translation of the leader RNA in the regulatory mechanism. Nonetheless the possibility remains that binding of the ribosome to the 5′ end of the mRNA still occurs in the U[+7]G mutant but is not detected *in vitro* because it does not result in the formation of a stable ternary complex with f-Met tRNA (which may be purely fortuitous). The data in Fig. 6 strongly suggest that RyhB1 pairing with its target sequence affects the structure of *iroN* mRNA in a way that increases the accessibility of the upstream site to ribosomal binding. To evaluate this interpretation and better define the upstream element we proceeded to analyze the effects of deletions in the initial portion of *iroN* mRNA.

An A/U-rich motif with dual silencer/enhancer activity at the 5′ end of iroN *mRNA*

The sequence at the beginning of *iroN* mRNA is A/U-rich and includes a motif, AAUAAU, that could participate in Hfq binding (Robinson *et al.*, 2014). If so, one might expect that removing this sequence might abolish or curb sRNA-mediated activation. To test this prediction, a portion of the A/U track, including the $(AAU)_2$ element, was removed as part of a 13 bp deletion (Δ[6-18], Fig. 5A) and the effects of this change on expression of the *iroN-lacZ* fusion were measured. As shown in Fig. 5D, the Δ[6-18] allele reduces *iroN* expression less than twofold. Significantly, this expression level does not result from partial sRNA activity since deleting *ryhB1* and *ryhB2* – or deleting *hfq* – causes ß-galactosidase levels to further decrease only slightly (Fig. 5D). Thus, removal of the A/U-rich sequence abolishes sRNA-dependent regulation and concomitantly increases the basal level of *iroN* expression in the absence of RyhB1 and RyhB2. The behaviour of Δ[6-18] is reproduced by another deletion, Δ[34-50], which removes the entirety of the sequence base-pairing with RyhB (Fig. 5A). Like Δ[6-18], Δ[34-50] increases the level of ß-galactosidase activity in the Δ*ryhB1* Δ*ryhB2* background (Fig. 5D). However, in this case the increase is less pronounced in the Δ*hfq* mutant suggesting that Hfq binding to the A/U-rich element has a positive effect on *iroN* expression (at least in this mutant) independently of sRNAs.

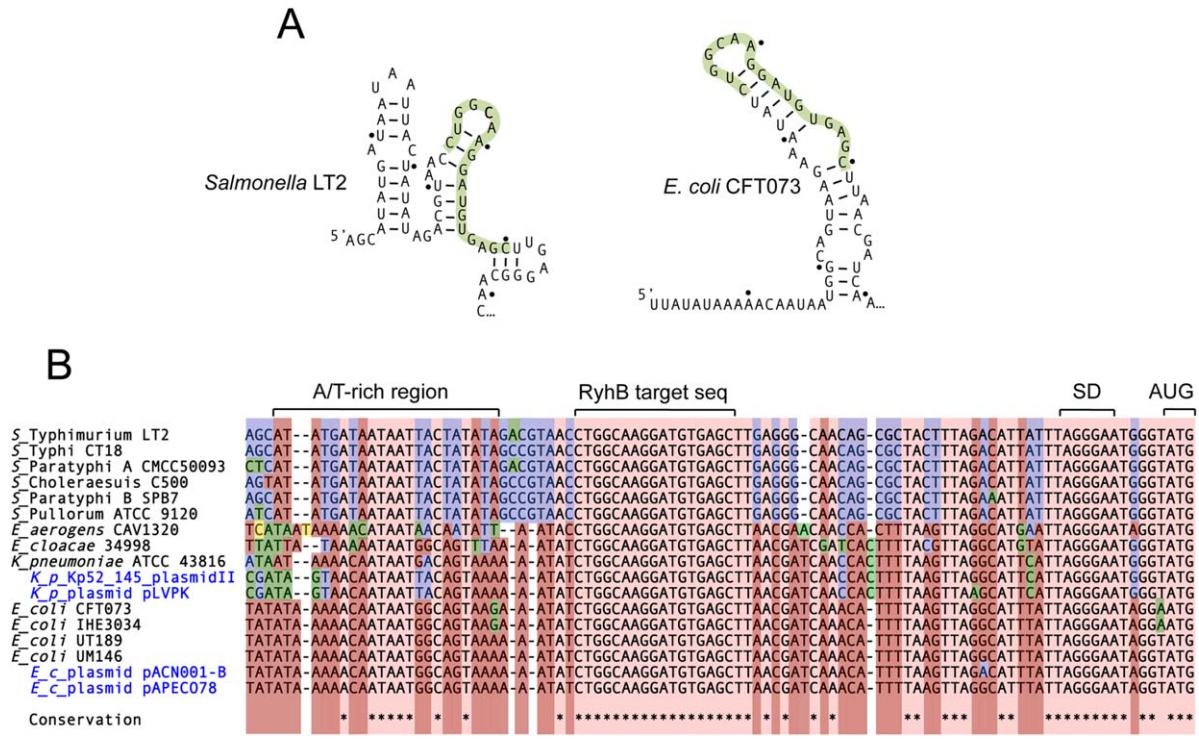

Fig. 7. A. Predicted secondary structure in the 5′ moieties of the *iroN* genes from *Salmonella enterica* and uropathogenic *Escherichia coli*. Shading denotes the RyhB1/2 target sequence.
B. Sequence alignment of *iroN* 5′ UTRs from representative enterobacterial strains or plasmids. The alignment was generated by the MultAlin on line tool (Corpet, 1988).

Altogether, these findings suggest that the sequence of the initial approximately 50 nucleotides of the *iroN* transcript exerts an inhibitory action on translation when RyhB1 or RyhB2 are absent. The sRNAs do not simply counteract the inhibition since the activity measured in the presence of RyhB1 is significantly higher than in either of the upstream deletion mutants. Analysis of the sequence of the initial 50 nt segment of the *iroN* mRNA with the NUPACK online tool (Zadeh *et al.*, 2011) reveals the possibility for the RyhB1 target sequence to participate in a secondary structure (Fig. 7A). The same is true for the RyhB target sequence in the *iroN* sequence of uropathogenic *Escherichia coli* (Fig. 7A). One might envision that either structure interferes with ribosomal binding at the upstream standby site (Espah Borujeni *et al.*, 2014) and that the establishment of the sRNA:mRNA hybrid reverses this effect by preventing the structure from forming.

Conservation of sequence motifs in iroN *5′ UTR*

While chromosomally located in all *Salmonella enterica* lineages (Bäumler *et al.*, 1998) and in uropathogenic *Escherichia coli* (Welch *et al.*, 2002), the *iroBCDE-iroN* gene cluster is also present in transmissible plasmids found in *Escherichia coli*, *Enterobacter* and in hypervirulent isolates of *Klebsiella pneumoniae* (Sorsa *et al.*, 2003; Di Lorenzo and Stork, 2014; Struve *et al.*, 2015). These findings underscore the relevance of this iron utilization system as a virulence determinant and corroborate the notion that it is acquired through horizontal transfer. Alignment of the sequences preceding the coding region of the *iroN* genes from different sources shows that the sequence of the RyhB-pairing segment and the A/U-richness of the 5′ terminal region are highly conserved (Fig. 7B). This strongly suggests that the regulatory mechanism identified in the present study is active in all bacteria that contain the locus. The ability to ‘plug into’ the regulatory circuitry of the host strain is likely to be a primary force driving the dissemination of this locus among different bacterial pathogens.

Discussion

We have shown that production of the salmochelin receptor, IroN, requires the post-transcriptional activation of *iroN* mRNA by either of two sRNA, RyhB1 or, somewhat less efficiently, RyhB2. Activation requires the establishment of a base-pair interaction between RyhB1/2 and a sequence

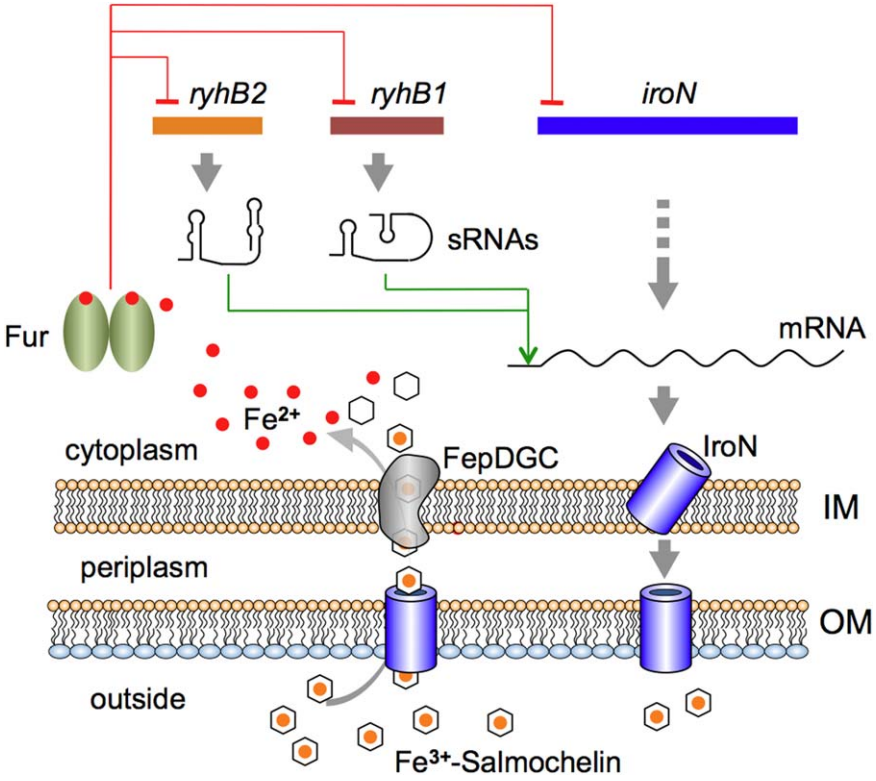

Fig. 8. Homeostatic mechanism for *iroN* regulation. The genes encoding regulatory sRNAs RyhB1 and RyhB2 and their positively regulated target, *iroN* mRNA, are all under the control of the Fur repressor. The three genes are transcribed under conditions where intracellular iron becomes limiting. However, *iroN* transcription is not sufficient to have the IroN protein made as this also requires that translation of *iroN* mRNA is activated by RyhB1 and RyhB2 (green arrows). Presumably, this regulatory 'and-gate' ensures that IroN is made only after alternative iron uptake sources are exhausted. Assembly of the IroN receptor in the outer membrane allows the Fe^{3+}-salmochelin complex to be imported into the cell. As the complex is degraded and Fe^{3+} is reduced, the intracellular concentration of Fe^{2+} raises. Fe^{2+} binding activates Fur, which restores repression of *ryhB1*, *ryhB2* and *iroN* (red blunt-end arrows).

in *iroN*'s 5′ UTR. Like the *iroN* gene (Bäumler *et al.*, 1998), the *ryhB1* and *ryhB2* genes are under the control of the Fur repressor and transcribed when iron levels become limiting (Massé and Gottesman, 2002; Padalon-Brauch *et al.*, 2008). Therefore, a direct implication of our findings is that the IroN protein can only be made provided that its gene is transcribed after RyhB1 and RyhB2 have sufficiently accumulated. A greater affinity of Fur for the *iroN* operator as compared to the *ryhB1/2* operator sites would explain such a hierarchy in the expression patterns. Presence of two Fur boxes in the *iroN* gene is generally consistent with this idea. Interestingly, one of the putative Fur boxes lies downstream from the transcription initiation site and corresponds to a portion of the RNA that plays a critical role in RyhB1/2-dependent regulation. Therefore, the same sequence element functions independently in transcriptional and post-transcriptional regulation. The requirement for two separate, albeit related conditions for production of IroN protein – transcriptional derepression and post-transcriptional activation – evokes parallels with logic AND-gate architecture, recently found to operate in another sRNA-mediated regulatory loop (Papenfort *et al.*, 2015). In the case of the *iroN* system, we hypothesize that the regulatory design has evolved to allow salmochelin uptake to occur as a last resource, when iron scavenging by enterochelin is unsuccessful, for example due to lipocalin-2 activity in the host environment. In allowing intracellular iron concentration to increase, IroN function will remove the condition responsible for the transcription of *ryhB1* and *ryhB2* genes in the first place (Fig. 8). This homeostatic pattern, whereby the action of the sRNA suppresses the signal responsible for its own synthesis, is not uncommon in sRNA-mediated regulation.

Both *iroN* and *ryhB2* genes are part of genomic islets acquired through horizontal transmission. At first, this might suggest that the two genes are linked in some specific way; however, our finding that RyhB2 plays a minor role in *iroN* regulation tentatively rules out the existence of such a link. This conclusion is strengthened by the observation that uropathogenic *Escherichia coli* harbors the *iroN* locus but does not carry a second *ryhB* gene. Conversely, *Salmonella bongori*, a species that diverged from *Salmonella enterica* early in evolution, carries *ryhB2* but not *iroN*. The latter observation

suggests that incorporation of the *ryhB2* islet in the *Salmonella* genome is an early event that preceded speciation and acquisition of the *iroN* islet. This leaves open the question as to why *Salmonella* species contain two *ryhB* homologues. One could speculate that RyhB1 and RyhB2, because of their sequence divergence, have dissimilar target ranges with subsets of mRNAs more efficiently recognized by one or the other of the two sRNAs. This, combined with reports indicating that *ryhB1* and *ryhB2* are differentially regulated in response to the growth phase transitions and oxidative stress (Calderón *et al*., 2014; Ortega *et al*., 2012) suggests that the two sRNAs make up distinct, albeit overlapping, regulatory networks. It seems possible that environmental conditions specific to the *Salmonella* lifestyle, in the host or outside, might favour the activity of one or the other of the two networks.

We have shown that the *iroN* mRNA, readily detectable in wild-type cells, disappears in cells lacking RyhB1 and RyhB2 due to rapid degradation through a pathway involving RNase E and PNPase. Observing a similar decay in cells that contain RyhB1 and RyhB2 and in which the *iroN* mRNA carries an initiation codon mutation indicated that translation is a major determinant of *iroN* mRNA stability. This, combined with the failure to detect increased RNase cleavage in the *iroN* 5′ UTR of *ryhB1/2* mutants, suggested that the two sRNAs act by stimulating *iroN* mRNA translation as opposed to directly protecting the mRNA against RNase activity. In previously known examples of sRNA-mediated translational activation, structural features in the region near the initiation codon are key determinants of the regulation. It was therefore surprising to find that the ability of RyhB1/2 to activate *iroN* was not significantly affected by replacing a segment of 28 nt preceding *iroN*'s initiator AUG with the corresponding region from other genes. Apparently, a different mechanism operates in *iroN*; a conclusion further corroborated by evidence that pointed to a role of the sequence at the 5′ end of mRNA in the regulatory mechanism.

The sequence of the initial portion of the *iroN* transcript is highly A/U-rich and includes an $(AAU)_2$ motif likely involved in Hfq binding. Indeed, removal of this sequence as part of a 13 nt deletion eliminates RyhB1/2-dependent activation almost completely. At the same time, the deletion causes a substantial increase in *iroN* mRNA expression in a Δ*ryhB1/2* strain. These findings suggest that the sequence at the 5′ end of *iroN* mRNA exerts an inhibitory effect on translation and that RyhB1 and RyhB2 act by countering this effect. Consistent with this picture, toeprint experiments revealed that pairing of RyhB1 with the *iroN* 5′UTR allows the 30S ribosomal subunit to form a ternary complex with f-Met tRNA and mRNA at an AUG triplet between +6 and +8. While subsequent work showed this complex to be physiologically irrelevant, the toeprint results nonetheless deliver an important piece of information in suggesting that RyhB1 can modify the structure of the 5′ terminal portion of the mRNA in a way that enhances ribosomal binding. Based on these findings, we propose that RyhB1/2 act by promoting the formation of an upstream standby site from where the ribosome can slide to the initiation region. Although novel, such a mechanism is not unexpected. The 30S ribosomal complex is thought to bind upstream 5′ UTR sequences through its platform domain (Marzi *et al*., 2007) and this type of interactions were recently shown to modulate translation initiation rates by over 100-fold (Espah Borujeni *et al*., 2014). Finding that sRNAs can hijack this regulatory potential is therefore not that surprising. Unfortunately, the exact nature of the putative standby site identified here remains elusive. We postulate that it spans the A/U rich segment at the 5′ end of iroN 5′ UTR possibly extending to include the left arms of the secondary structures depicted in Fig. 7A. If so, the positive role of RyhB1(2) might result from the fact that its pairing with the mRNA would break down the secondary structure and allow 5′ end sequence to adopt a conformation more suitable for ribosome binding.

A/U-rich sequences are also binding sites for protein S1, a loosely associated ribosomal component known to modulate translation initiation in mRNAs with structured leader sequences (Hajnsdorf and Boni, 2012). Various lines of evidence, beginning with the study of phage Qß replicase (Blumenthal and Carmichael, 1979), point to the existence of a functional link between S1 and Hfq. Intriguingly, S1 but not Hfq, was pulled down in high affinity chromatography pull-down assays with the RyhB RNA sequence as bait (Windbichler *et al*., 2008), suggesting that RyhB binds S1 with greater affinity than Hfq. Could all three factors, RyhB1, Hfq and S1, connect in the regulation of iroN mRNA translation? Clearly, further work is needed to answer this question and define the nature of the regulatory mechanism.

Experimental procedures

Bacterial strains and culture conditions

Strains used in this work are derived from either of two strains of *Salmonella enterica* serovar Typhimurium: strain MA3409, a derivative of strain LT2 (Lilleengen, 1948) cured for the Gifsy-1 prophage (Figueroa-Bossi *et al*., 1997) and strain ATCC14028 (Fields *et al*., 1986). The genotypes of the relevant strains used are listed in Supporting Information Table S1. Bacteria were cultured at 37°C in liquid media or in media solidified by the addition of 1.5% Difco agar. LB broth (Bertani, 2004) was used as complex medium. Carbon-free medium (NCE) (Maloy and Roth, 1983), supplemented with 0.2% glycerol or 0.2% lactose was used as

minimal medium. Antibiotics (Sigma-Aldrich) were included at the following final concentrations: chloramphenicol, 10 μg ml^{-1}; kanamycin monosulphate, 50 μg ml^{-1}; sodium ampicillin 100 μg ml^{-1}; spectinomycin dihydrochloride, 80 μg ml^{-1}; tetracycline hydrochloride, 25 μg ml^{-1}. MacConkey agar plates containing 1% lactose (Macconkey, 1905) were used to monitor *lacZ* expression in bacterial colonies. Liquid cultures were grown in New Brunswick gyratory shakers and growth was monitored by measuring the optical density at 600 nm with a Shimazu UV-mini 1240 spectrophotometer.

Genetic techniques

Generalized transduction was performed using the high-frequency transducing mutant of phage P22, HT 105/1 *int-201* (Schmieger, 1972) as described (Lemire *et al.*, 2011). Chromosomal engineering (recombineering) was carried out by the λ *red* recombination method (Datsenko and Wanner, 2000; Murphy *et al.*, 2000; Yu *et al.*, 2000) implemented as in (Datsenko and Wanner, 2000). Chromosomal *lacZ* gene fusions were constructed with the two-step procedure of (Ellermeier *et al.*, 2002). Marker-free scarless mutagenesis was carried out as described (Figueroa-Bossi and Bossi, 2015). Unless specified otherwise, the latter protocol was used for introducing point mutations in the chromosome. Donor DNA fragments used in all of the above procedures were generated by the polymerase-chain reaction (PCR) using plasmid DNA or chromosomal DNA or DNA oligonucleotides as templates. Amplified fragments were electroporated into appropriate strains harboring the conditionally replicating plasmid pKD46, which carries the λ *red* operon under the control of the P^{BAD} promoter (Datsenko and Wanner, 2000). Bacteria carrying pKD46 were grown at 30°C in the presence of ampicillin. Arabinose (10 mM) was added 3 hours prior to preparation of electrocompetent cells. Electroporation was carried out using a Bio-Rad MicroPulser under the conditions specified by the manufacturer. Recombinant colonies were selected on LB plates containing the appropriate selection agent. Constructs were verified by PCR and DNA sequence analysis (performed by GATC company). DNA oligonucleotides used as PCR primers in the above constructions are listed in Supporting Information Table S2. The correspondence between mutant alleles and primer/template combinations is detailed in Supporting Information Table S3.

Measurement of β-galactosidase activity

β-galactosidase activity was assayed in toluene-permeabilized cells as described in (Miller, 1992) and is expressed in Miller units or as percentage of the activity measured in the wild-type strain in the same experiment. Typically, measurements were performed on duplicate or triplicate cultures grown in late exponential phase ($OD_{600} \approx 0.7$). Standard deviations were generally less than 5% of the mean.

OMP preparation

Salmonella OMP fraction was purified by the method of (Santiviago *et al.*, 2003) with minor modifications. Briefly, bacteria were grown in 25 ml of LB or NCE-glycerol medium to $O.D_{600}$ of 0.35 and collected by centrifugation. Pellet was resuspended in 1 ml of 10 mM Tris pH 8.0 and sonicated on ice, using 3 pulses of 20 s with 30 s resting intervals (Vibra Cell sonicator equipped with microtip, Sonics & Materials Inc). Lysate was centrifuged at 7,000 rpm for 5 min, supernatant recovered and centrifuged at 13,000 r.p.m. for 45 min at 20°C in a thermo-regulated microcentrifuge. Pellet was resuspended in 0.5 ml of freshly made 10 mM Tris-HCl pH 8.0, 10 mM $MgCl_2$, 2% (v/v) Triton X-100. The suspension was incubated at 37°C for 30 min, then centrifuged at 13,000 rpm for 45 min at 20°C. The pellet was resuspended in 50 to 100 μl of 100 mM Tris-HCl pH 8.0, 2% SDS and kept at −20°C. Proteins were fractionated by SDS-PAGE and revealed by Coomassie blue staining.

MALDI Peptide Mass Fingerprinting. Performed by the Service for Identification and Characterization of Proteins by Mass Spectrometry of the 'SICaPS' Platform of the CNRS in Gif-sur-Yvette, France. Briefly, protein bands were excised from the gel and extensively washed with CH_3CN and 25 mM NH_4HCO_3. The gel slices were treated with 100 μl 10 mM DTT at 57°C for 30 minutes. The DTT was removed and 100 μl of 55 mM iodoacetamide was added for cysteine carbamidomethylation. The reaction was allowed to proceed for 30 min at room temperature. The supernatant was removed, the washing procedure was repeated and the slices were dried. We added 20 μl of 10 ng/μl Trypsin (Promega) diluted in 25 mM NH_4HCO_3 and the mixture was incubated overnight at room temperature. Peptides were extracted in 60% acetonitrile and 0.1% (v/v) formic acid and 0.5 μl were mixed with an equal volume of α-cyano-4-hydroxycinnamic acid (10 mg/ml, 50% CH_3CN; Sigma-Aldrich). Crystals were obtained using the dried droplet method and Trypsin-generated peptide mixtures were analysed in positive reflectron mode with the Voyager-DE STR MALDI-TOF mass spectrometer (ABSCIEX) – 500 mass spectra were averaged per spot. MALDI peptide mass fingerprinting (PMF) spectra were internally calibrated with autolytic peptides of trypsin. Peak lists were generated by the Data Explorer software (Applied Biosystems) and processed data were submitted to the Profound software (The Rockefeller University) using the following parameters: nrNCBI database, digest reagent Trypsin, cysteine carbamidomethylation and oxidation (methionine and tryptophan) were considered respectively a complete and variable modification and peptide mass tolerance was set at 20 ppm.

RNA extraction and Northern blot analysis

RNA was prepared by the acid-hot-phenol method from exponentially growing cells (OD_{600} of 0.35) as previously described (Figueroa *et al.*, 1991). Total RNA was estimated from the value of the OD at 260nm. For Northern analysis, 7.5 μg of total RNA were separated under denaturing conditions either by 8% polyacrylamide-8M urea in TBE (Tris-borate-EDTA pH 8.3) buffer or by 1.3% agarose-2.2 M formaldehyde gel electrophoresis in MOPS ([N-morpholino] propanesulfonic acid-sodium acetate-EDTA pH7.0) buffer. For polyacrylamide gels, transfer of the RNA onto Hybond-N^+ membrane (Amersham), was performed with a semidry

electrotransfer apparatus (Transblot SD; BioRad); in the case of agarose gels, transfer to the same support was done using a vacuum blotter (Boekel/Appligene) after mild denaturation treatment in 50 mM NaOH, 10 mM NaCl. RNA was crosslinked to membrane by UV irradiation (Statagene UV Stratalinker 2400). DNA Membranes were hybridized to DNA oligonucleotides probes (Supporting Information Table S2) as follows: 5 pmol of oligonucleotide were 5′ end-labelled using 10 U of T4 polynucleotide kinase (New England Biolabs) and 30 mCi of [γ-^{32}P]ATP (3,000 mCi mmol^{-1}, Hartmann Analytic). Unincorporated radioactivity was eliminated by passage through Micro-Bio Spin 6 chromatography columns (BioRad). Hybridization was carried out in Ambion Oligonucleotide Hybridization Buffer at 45–50°C following Ambion's protocol. RNA was analysed by Phosphorimaging using ImageQuant software.

Western blot analysis

Strains carrying 3xFLAG fusion proteins were grown in 1.5 ml cultures to stationary phase and processed for the immunodetection of the 3xFLAG epitope using anti-FLAG m2 monoclonal antibodies (Sigma) and horseradish peroxidase-conjugated goat anti-mouse IgG (Sigma) as described (Uzzau *et al*., 2001).

Primer extension

Reverse transcriptase reactions (enzyme Superscript II from Invitrogen) were carried out using 5 μg of bulk RNA and ^{32}P-labelled primer ppH09 (Supporting Information Table S2). The same DNA primer was used for the sequencing reactions. Reactions were performed with the *fmol* DNA Cycle Sequencing System from Promega, according to the manufacturer's protocol. Reaction products were fractionated on a 10% polyacrylamide-8 M urea gel.

Toeprint assays

Toeprinting reactions were carried out as described by Darfeuille *et al*. (2007) with minor modifications. RyhB and the portion of iroN RNA from +1 to +188 were synthesized *in vitro* from T7 DNA templates generated by PCR amplification of chromosomal DNA. 2 pmol of RNA were annealed with 5′end-labelled primer (0.1 pmol) in 20 mM Tris-acetate [pH7.6], 200 mM potassium acetate and 2 mM DTT for 1 min at 90°C and chilled in ice for 5 min. Then, all dNTPs (final concentration 0.8 mM each), Mg Acetate (10 mM final) were added; this was followed by preincubation with 2.6 pmol of 30S ribosomal subunit at 37°C for 5 min. In samples containing RyhB1, 110 pmol of sRNA were added prior to the addition of the 30S ribosomal subunit and the preincubation step. After the 5 min period, 10 pmol of tRNA^{fMet} were added and preincubation at 37°C continued for 15 additional min. Finally, Reverse Transcriptase (Superscript II, Invitrogen, 200U) was added and samples incubated for 15 min at 37°C. Following phenol chloroform extraction and ethanol precipitation, resuspended samples were loaded onto a 10% polyacrylamide-8 M urea gel along with the sequencing reaction samples generated with the same primer.

Acknowledgements

We are grateful to Fabien Darfeuille for valuable advice on the toeprint protocol and to Dominique Fourmy and Satoko Yoshizawa for the gift of purified 30S ribosomal subunits used for the toeprint analysis. We also thank David Cornu of the SiCaPS (I2BC) platform for providing the protocol of the MALDI PMF analysis. This work was funded by grants ANR-BLAN07-1_187785 (to L.B.) and ANR-3-BSV3-0005 (to N.F.B.) from the French National Research Agency (ANR). N.V. acknowledges support from ASM International Fellowship program for Latin America and the Caribbean (October 2011 session). Travel support from ECOS Sud-Conicyt France-Chile joint grant C07B03 to L.B. and G.M. is also acknowledged.

References

Bandyra, K.J., Said, N., Pfeiffer, V., Gorna, M.W., Vogel, J., and Luisi, B.F. (2012) The seed region of a small RNA drives the controlled destruction of the target mRNA by the endoribonuclease RNase E. *Mol Cell* **47**: 943–953.

Bäumler, A.J., Norris, T.L., Lasco, T., Voight, W., Reissbrodt, R., Rabsch, W., and Heffron, F. (1998) IroN, a novel outer membrane siderophore receptor characteristic of *Salmonella enterica*. *J Bacteriol* **180**: 1446–1453.

Bertani, G. (2004) Lysogeny at mid-twentieth century: P1, P2, and other experimental systems. *J Bacteriol* **186**: 595–600.

Bleuel, C., Grosse, C.,Taudte, N., Scherer, J., Wesenberg, D., Krauss, G.J., *et al*. (2005) TolC is involved in enterobactin efflux across the outer membrane of *Escherichia coli*. *J Bacteriol* **187**: 6701–6707.

Blumenthal, T.and Carmichael, G.G. (1979) RNA replication: function and structure of Qbeta-replicase. *Annu Rev Biochem* **48**: 525–548.

Braun, V., and Braun, M. (2002) Active transport of iron and siderophore antibiotics. *Curr Opin Microbiol* **5**: 194–201.

Braun, V., and Hantke, K. (2011) Recent insights into iron import by bacteria. *Curr Opin Chem Biol* **15**: 328–334.

Buchanan, S.K., Smith, B.S., Venkatramani, L., Xia, D., Esser, L., Palnitkar, M., *et al*. (1999) Crystal structure of the outer membrane active transporter FepA from *Escherichia coli*. *Nat Struct Biol* **6**: 56–63.

Calderón, I.L., Morales, E.H., Collao, B., Calderón, P.F., Chahuan, C.A., Acuna, L.G. *et al*. (2014) Role of Salmonella Typhimurium small RNAs RyhB-1 and RyhB-2 in the oxidative stress response. *Res Microbiol* **165**: 30–40.

Carpenter, B.M., Whitmire, J.M., and Merrell, D.S. (2009) This is not your mother's repressor: the complex role of fur in pathogenesis. *Infect Immun* **77**: 2590–2601.

Corpet, F. (1988) Multiple sequence alignment with hierarchical clustering. *Nucleic Acids Res* **16**: 10881–10890.

Crosa, J.H., and Walsh, C.T. (2002) Genetics and assembly line enzymology of siderophore biosynthesis in bacteria. *Microbiol Mol Biol Rev* **66**: 223–249.

Crouch, M.L., Castor, M., Karlinsey, J.E., Kalhorn, T., and Fang, F.C. (2008) Biosynthesis and IroC-dependent export of the siderophore salmochelin are essential for virulence of *Salmonella enterica* serovar Typhimurium. *Mol Microbiol* **67**: 971–983.

Darfeuille, F., Unoson, C., Vogel, J., and Wagner, E.G. (2007) An antisense RNA inhibits translation by competing with standby ribosomes. *Mol Cell* **26**: 381–392.

Datsenko, K.A., and Wanner, B.L. (2000) One-step inactivation of chromosomal genes in *Escherichia coli* K-12 using PCR products. *Proc Natl Acad Sci U S A* **97**: 6640–6645.

De Lay, N., and Gottesman, S. (2011) Role of polynucleotide phosphorylase in sRNA function in *Escherichia coli*. *RNA* **17**: 1172–1189.

De Lay, N., Schu, D.J., and Gottesman, S. (2013) Bacterial small RNA-based negative regulation: Hfq and its accomplices. *J Biol Chem* **288**: 7996–8003.

Deana, A., Celesnik, H., and Belasco, J.G. (2008) The bacterial enzyme RppH triggers messenger RNA degradation by 5′ pyrophosphate removal. *Nature* **451**: 355–358.

Di Lorenzo, M., and Stork, M. (2014) Plasmid-Encoded Iron Uptake Systems. *Microbiol Spectr* **2**.

Dreyfus, M. (2009) Killer and protective ribosomes. *Prog Mol Biol Transl Sci* **85**: 423–466.

Ellermeier, C.D., Janakiraman, A., and Slauch, J. M. (2002) Construction of targeted single copy *lac* fusions using lambda Red and FLP-mediated site-specific recombination in bacteria. *Gene* **290**: 153–161.

Ellermeier, J.R., and Slauch, J.M. (2008) Fur regulates expression of the *Salmonella* pathogenicity island 1 type III secretion system through HilD. *J Bacteriol* **190**: 476–486.

Espah Borujeni, A., Channarasappa, A.S., and Salis, H.M. (2014) Translation rate is controlled by coupled trade-offs between site accessibility, selective RNA unfolding and sliding at upstream standby sites. *Nucleic Acids Res* **42**: 2646–2659.

Fields, P.I., Swanson, R.V. Haidaris, C.G., and Heffron, F. (1986) Mutants of *Salmonella typhimurium* that cannot survive within the macrophage are avirulent. *Proc Natl Acad Sci U S A* **83**: 5189–5193.

Figueroa, N., Wills, N., and Bossi, L. (1991) Common sequence determinants of the response of a prokaryotic promoter to DNA bending and supercoiling. *EMBO J* **10**: 941–949.

Figueroa-Bossi, N., and Bossi, L. (2015) Recombineering applications for the mutational analysis of bacterial RNA-binding proteins and their sites of action. *Methods Mol Biol* **1259**: 103–116.

Figueroa-Bossi, N., Coissac, E. Netter, P., and Bossi, L. (1997) Unsuspected prophage-like elements in *Salmonella typhimurium*. *Mol Microbiol* **25**: 161–173.

Figueroa-Bossi, N., Valentini, M., Malleret, L., Fiorini, F., and Bossi, L. (2009) Caught at its own game: regulatory small RNA inactivated by an inducible transcript mimicking its target. *Genes Dev* **23**: 2004–2015.

Fischbach, M.A., Lin, H., Liu D.R., and Walsh, C.T. (2006) How pathogenic bacteria evade mammalian sabotage in the battle for iron. *Nat Chem Biol* **2**: 132–138.

Flo, T.H., Smith, K.D., Sato, S., Rodriguez, D.J., Holmes, M.A., Strong, R.K., *et al*. (2004) Lipocalin 2 mediates an innate immune response to bacterial infection by sequestrating iron. *Nature* **432**: 917–921.

Frohlich, K.S., Papenfort, K., Fekete, A., and Vogel, J. (2013) A small RNA activates CFA synthase by isoform-specific mRNA stabilization. *EMBO J* **32**: 2963–2979.

Furrer, J.L., Sanders, D.N., Hook-Barnard, I.G., and McIntosh, M.A. (2002) Export of the siderophore enterobactin in *Escherichia coli*: involvement of a 43 kDa membrane exporter. *Mol Microbiol* **44**: 1225–1234.

Gottesman, S., and Storz, G. (2011) Bacterial small RNA regulators: versatile roles and rapidly evolving variations. *Cold Spring Harb Perspect Biol* doi: 10.1101/cshperspect.a003798.

Hajnsdorf, E., and Boni, I.V. (2012) Multiple activities of RNA-binding proteins S1 and Hfq. *Biochimie* **94**: 1544–1553.

Hantke, K. (2001) Iron and metal regulation in bacteria. *Curr Opin Microbiol* **4**: 172–177.

Hantke, K., Nicholson, G., Rabsch, W., and Winkelmann, G. (2003) Salmochelins, siderophores of *Salmonella enterica* and uropathogenic *Escherichia coli* strains, are recognized by the outer membrane receptor IroN. *Proc Natl Acad Sci U S A* **100**: 3677–3682.

Hartz, D., McPheeters, D.S., Traut, R., and Gold, L. (1988) Extension inhibition analysis of translation initiation complexes. *Methods Enzymol* **164**: 419–425.

Ikeda, Y., Yagi, M., Morita, T., and Aiba, H. (2011) Hfq binding at RhlB-recognition region of RNase E is crucial for the rapid degradation of target mRNAs mediated by sRNAs in *Escherichia coli*. *Mol Microbiol* **79**: 419–432.

Jacques, J.F., Jang, S., Prevost, K., Desnoyers, G., Desmarais, M., Imlay J., and Massé, E. (2006) RyhB small RNA modulates the free intracellular iron pool and is essential for normal growth during iron limitation in *Escherichia coli*. *Mol Microbiol* **62**: 1181–1190.

Kim, J.N., and Kwon, Y.M. (2013) Genetic and phenotypic characterization of the RyhB regulon in *Salmonella* Typhimurium. *Microbiol Res* **168**: 41–49.

Leclerc, J.M., Dozois, C.M., and Daigle, F. (2013) Role of *Salmonella enterica* serovar Typhi Fur regulator and small RNAs RfrA and RfrB in iron homeostasis and interaction with host cells. *Microbiology* **159**: 591–602.

Lemire, S., Figueroa-Bossi, N., and Bossi, L. (2011) Bacteriophage crosstalk: coordination of prophage induction by trans-acting antirepressors. *PLoS Genet* **7**: e1002149.

Lilleengen, K. (1948) Typing of *Salmonella typhimurium* by means of bacteriophage. *Acta Pathol. Microbiol. Scand.* **77**: 2–125.

Lin, H., Fischbach, M.A., Liu, D.R., and Walsh, C.T. (2005) In vitro characterization of salmochelin and enterobactin trilactone hydrolases IroD, IroE, and Fes. *J Am Chem Soc* **127**: 11075–11084.

Macconkey, A. (1905) Lactose-Fermenting Bacteria in Faeces. *J Hyg (Lond)* **5**: 333–379.

Maloy, S.R., and Roth, J.R. (1983) Regulation of proline utilization in *Salmonella typhimurium*: characterization of *put*:: Mu d(Ap, *lac*) operon fusions. *J Bacteriol* **154**: 561–568.

Mandin, P., and Guillier, M. (2013) Expanding control in bacteria: interplay between small RNAs and transcriptional regulators to control gene expression. *Curr Opin Microbiol* **16**: 125–132.

Marzi, S., Myasnikov, A.G., Serganov, A., Ehresmann, C., Romby, P., Yusupov, M., and Klaholz, B.P. (2007) Structured mRNAs regulate translation initiation by binding to the platform of the ribosome. *Cell* **130**: 1019–1031.

Massé, E., Escorcia, F.E., and Gottesman, S. (2003) Coupled degradation of a small regulatory RNA and its mRNA targets in *Escherichia coli*. *Genes Dev* **17**: 2374–2383.

Massé, E., and Gottesman, S. (2002) A small RNA regulates the expression of genes involved in iron metabolism in *Escherichia coli*. *Proc Natl Acad Sci U S A* **99**: 4620–4625.

Massé, E., Salvail, H., Desnoyers, G., and Arguin, M. (2007) Small RNAs controlling iron metabolism. *Curr Opin Microbiol* **10**: 140–145.

Massé, E., Vanderpool, C.K., and Gottesman, S. (2005) Effect of RyhB small RNA on global iron use in *Escherichia coli*. *J Bacteriol* **187**: 6962–6971.

McCullen, C.A., Benhammou, J.N., Majdalani, N., and Gottesman, S. (2010) Mechanism of positive regulation by DsrA and RprA small noncoding RNAs: pairing increases translation and protects rpoS mRNA from degradation. *J Bacteriol* **192**: 5559–5571.

Miller, J.H., (1992) *A Short Course in Bacterial Genetics. A Laboratory Manual and Handbook for Escherichia coli and Related Bacteria*. Cold Spring Harbor Laboratory Press, Cold Spring Harbor, New York.

Morita, T., Maki, K., and Aiba, H. (2005) RNase E-based ribonucleoprotein complexes: mechanical basis of mRNA destabilization mediated by bacterial noncoding RNAs. *Genes Dev* **19**: 2176–2186.

Morita, T., Mochizuki Y., and Aiba, H. (2006) Translational repression is sufficient for gene silencing by bacterial small noncoding RNAs in the absence of mRNA destruction. *Proc Natl Acad Sci U S A* **103**: 4858–4863.

Muller, S.I., Valdebenito, M., and Hantke, K. (2009) Salmochelin, the long-overlooked catecholate siderophore of *Salmonella*. *Biometals* **22**: 691–695.

Murphy, K.C., Campellone, K.G., and Poteete, A.R. (2000) PCR-mediated gene replacement in *Escherichia coli*. *Gene* **246**: 321–330.

Notredame, C., Higgins, D.G., and Heringa, J. (2000) T-Coffee: a novel method for fast and accurate multiple sequence alignment. *J Mol Biol* **302**: 205–217.

Ortega, A., Gonzalo-Asensio, J., and Garcia-Del Portillo, F. (2012) Dynamics of *Salmonella* small RNA expression in non-growing bacteria located inside eukaryotic cells. *RNA Biol* **9**: 469–488.

Padalon-Brauch, G., Hershberg, R., Elgrably-Weiss, M., Baruch, K., Rosenshine, I., Margalit, H., and Altuvia, S. (2008) Small RNAs encoded within genetic islands of *Salmonella typhimurium* show host-induced expression and role in virulence. *Nucleic Acids Res* **36**: 1913–1927.

Papenfort, K., Espinosa, E., Casadesus, J., and Vogel, J. (2015) Small RNA-based feedforward loop with AND-gate logic regulates extrachromosomal DNA transfer in *Salmonella*. *Proc Natl Acad Sci U S A* **112**: E4772–E4781.

Papenfort, K., Sun, Y., Miyakoshi, M.,Vanderpool, C.K., and Vogel, J. (2013) Small RNA-mediated activation of sugar phosphatase mRNA regulates glucose homeostasis. *Cell* **153**: 426–437.

Papenfort, K., and Vanderpool, C.K. (2015) Target activation by regulatory RNAs in bacteria. *FEMS Microbiol Rev* **39**: 362–378.

Porcheron, G., Habib, R., Houle, S., Caza, M., Lepine, F., Daigle, F., *et al*. (2014) The small RNA RyhB contributes to siderophore production and virulence of uropathogenic *Escherichia coli*. *Infect Immun* **82**: 5056–5068.

Prevost, K., Desnoyers, G., Jacques, J.F., Lavoie, F., and Massé, E. (2011) Small RNA-induced mRNA degradation achieved through both translation block and activated cleavage. *Genes Dev* **25**: 385–396.

Prevost, K., Salvail, H., Desnoyers, G., Jacques, J.F., Phaneuf, E., and Massé, E. (2007) The small RNA RyhB activates the translation of *shiA* mRNA encoding a permease of shikimate, a compound involved in siderophore synthesis. *Mol Microbiol* **64**: 1260–1273.

Raffatellu, M., George, M.D., Akiyama, Y., Hornsby, M.J., Nuccio, S.P., Paixao, T.A., *et al*. (2009) Lipocalin-2 resistance confers an advantage to *Salmonella enterica* serotype Typhimurium for growth and survival in the inflamed intestine. *Cell Host Microbe* **5**: 476–486.

Robinson, K.E., Orans, J., Kovach, A.R., Link, T.M., and Brennan, R.G. (2014) Mapping Hfq-RNA interaction surfaces using tryptophan fluorescence quenching. *Nucleic Acids Res* **42**: 2736–2749.

Salvail, H., Caron, M.P., Belanger, J., and Massé, E. (2013) Antagonistic functions between the RNA chaperone Hfq and an sRNA regulate sensitivity to the antibiotic colicin. *EMBO J* **32**: 2764–2778.

Salvail, H., Lanthier-Bourbonnais, P., Sobota, J.M., Caza, M., Benjamin, J.A., Mendieta, M.E. *et al*. (2010) A small RNA promotes siderophore production through transcriptional and metabolic remodeling. *Proc Natl Acad Sci U S A* **107**: 15223–15228.

Santiviago, C.A., Toro, C.S., Hidalgo, A.A., Youderian, P., and Mora, G.C. (2003) Global regulation of the *Salmonella enterica* serovar typhimurium major porin, OmpD. *J Bacteriol* **185**: 5901–5905.

Schaible, U.E., and Kaufmann, S.H. (2004) Iron and microbial infection. *Nat Rev Microbiol* **2**: 946–953.

Schmieger, H. (1972) Phage P22-mutants with increased or decreased transduction abilities. *Mol Gen Genet* **119**: 75–88.

Soper, T., Mandin, P., Majdalani, N., Gottesman S., and Woodson, S.A. (2010) Positive regulation by small RNAs and the role of Hfq. *Proc Natl Acad Sci U S A* **107**: 9602–9607.

Sorsa, L.J., Dufke, S., Heesemann, J., and Schubert, S. (2003) Characterization of an *iroBCDEN* gene cluster on a transmissible plasmid of uropathogenic *Escherichia coli*: evidence for horizontal transfer of a chromosomal virulence factor. *Infect Immun* **71**: 3285–3293.

Struve, C., Roe, C.C., Stegger, M., Stahlhut, S.G., Hansen, D.S., Engelthaler, D.M., *et al*. (2015) Mapping the Evolution of Hypervirulent *Klebsiella pneumoniae*. *MBio* **6**: e00630–15.

Tsolis, R.M., Bäumler, A.J., Stojiljkovic, I., and Heffron, F. (1995) Fur regulon of *Salmonella typhimurium*: identification of new iron-regulated genes. *J Bacteriol* **177**: 4628–4637.

Uzzau, S., Figueroa-Bossi, N., Rubino, S., and Bossi, L. (2001) Epitope tagging of chromosomal genes in *Salmonella*. *Proc Natl Acad Sci U S A* **98**: 15264–15269.

Vogel, J., and Luisi, B.F. (2011) Hfq and its constellation of RNA. *Nat Rev Microbiol* **9**: 578–589.

Wandersman, C., and Delepelaire, P. (2004) Bacterial iron sources: from siderophores to hemophores. *Annu Rev Microbiol* **58**: 611–647.

Welch, R.A., Burland, V. Plunkett, G. 3rd, Redford, P. Roesch, P. Rasko, D. *et al*. (2002) Extensive mosaic structure revealed by the complete genome sequence of

uropathogenic *Escherichia coli*. *Proc Natl Acad Sci U S A* **99**: 17020–17024.
Windbichler, N., von Pelchrzim, F., Mayer, O., Csaszar, E., and Schroeder, R. (2008) Isolation of small RNA-binding proteins from *E. coli*: evidence for frequent interaction of RNAs with RNA polymerase. *RNA Biol* **5**: 30–40.
Yang, Q., Figueroa-Bossi, N., and Bossi, L. (2014) Translation enhancing ACA motifs and their silencing by a bacterial small regulatory RNA. *PLoS Genet* **10**: e1004026.
Yu, D., Ellis, H.M., Lee, E.C., Jenkins, N.A., Copeland, N.G., and Court, D.L. (2000) An efficient recombination system for chromosome engineering in *Escherichia coli*. *Proc Natl Acad Sci U S A* **97**: 5978–5983.
Zadeh, J.N., Steenberg, C.D., Bois, J.S., Wolfe, B.R., Pierce, M.B., Khan, A.R., *et al*. (2011) NUPACK: analysis and design of nucleic acid systems. *J Comput Chem* **32**: 170–173.
Zhu, M., Valdebenito, M., Winkelmann, G., and Hantke, K. (2005) Functions of the siderophore esterases IroD and IroE in iron-salmochelin utilization. *Microbiology* **151**: 2363–2372.
Zuker, M. (2003) Mfold web server for nucleic acid folding and hybridization prediction. *Nucleic Acids Res* **31**: 3406–3415.

Supporting information

Additional supporting information may be found in the online version of this article at the publisher's web-site.